Histol Histopathol (2023) 38: 571-584

http://www.hh.um.es

Histology and Histopathology
From Cell Biology to Tissue Engineering

ORIGINAL ARTICLE **Open Access**

Circ_0085616 contributes to the radio-resistance and progression of cervical cancer by targeting miR-541-3p/ARL2 signaling

Yan Tang[1], Lei Zhou[2] and Lili Liu[1]

[1]Department of Gynecology and Obstetrics and [2]Allergy and Clinical Immunology Research Centre, First Affiliated Hospital of Jinzhou Medical University, Jinzhou City, Liaoning Province, PR China

Summary. Background. Circular RNAs (circRNAs) play crucial regulatory roles in cancer progression and the development of radio-resistance. Here, we intended to explore the role of circ_0085616 in cervical cancer progression and its associated mechanism.

Methods. Colony formation assay was employed to analyze the radio-resistance and proliferation of cervical cancer cells. Cell proliferation ability was also assessed by 5-ethynyl-2'-deoxyuridine (EdU) assay. Cell apoptosis was analyzed by flow cytometry. Tube formation assay was performed to analyze cell angiogenesis ability. Transwell assays were conducted to measure cell migration and invasion abilities. Dual-luciferase reporter assay was utilized to verify the target relationships. Xenograft mice model was used to analyze the role of circ_0085616 in tumor growth *in vivo*.

Results. Circ_0085616 expression was elevated in cervical cancer tissues and cell lines. Circ_0085616 interference suppressed the radio-resistance, proliferation, tube formation, migration, and invasion and elevated the apoptosis rate of cervical cancer cells. Circ_0085616 acted as a sponge for microRNA-541-3p (miR-541-3p), and miR-541-3p was negatively regulated by circ_0085616 in cervical cancer cells. Circ_0085616 absence-induced changes in the behaviors of cervical cancer cells were largely overturned by anti-miR-541-3p. miR-541-3p negatively regulated ADP ribosylation factor like GTPase 2 (ARL2) expression by binding to its 3' untranslated region (3'UTR). miR-541-3p mimic-induced effects were largely reversed by pcDNA-ARL2 in cervical cancer cells. Circ_0085616 positively regulated ARL2 expression by sequestering miR-541-3p. Circ_0085616 absence significantly inhibited the tumor growth *in vivo*.

Conclusion. Circ_0085616 contributed to the radio-resistance and progression of cervical cancer partly through mediating the miR-541-3p/ARL2 axis.

Key words: Cervical cancer, Radio-resistance, circ_0085616, miR-541-3p, ARL2

Corresponding Author: Lili Liu, Department of Gynecology and Obstetrics, First Affiliated Hospital of Jinzhou Medical University, No.2, section 5, Renmin Street, Guta District, Jinzhou 121000, Liaoning Province, PR China. e-mail: jzmu_liulili@163.com

DOI: 10.14670/HH-18-541

Introduction

Surgery, radiotherapy, and chemotherapy remain the major therapeutic strategies for patients with cervical cancer (Li et al., 2016). However, the development of radio-resistance limits the effectiveness of current treatment for cervical cancer (Masadah et al., 2021). It is crucial to investigate the molecular mechanism underlying cervical cancer development to overcome the radio-resistance of cancer cells.

Circular RNAs (circRNAs) are reported to be crucial regulators in cancer pathogenesis (Kristensen et al., 2018). Moreover, accumulating documents demonstrated that circRNAs work as microRNA (miRNA) sponges to regulate the progression of cancers, including cervical cancer (Guo et al., 2019; Tang et al., 2019). Circ_0085616 is located at chr8 and is derived from the ASAP1 gene. A previous study showed that circ_0085616 was upregulated in hepatocellular carcinoma tissues, and its downregulation inhibited cancer cell proliferation and migration, which might be dependent on the regulation of miR-326/miR-532-5p-MAPK1/CSF-1 pathway (Hu et al., 2020). Besides, circ_0085616 is reported to be up-regulated in cervical cancer on the basis of heatmap data (Shao et al., 2020). Furthermore, a previous study demonstrated that circ_0085616 contributed to cervical cancer progression through the regulation of the miR-503-5p/ATXN7L3 pathway (Lin et al., 2020). MiR-541-3p is reported to exert an anti-tumor function in several malignancies (Lu et al., 2016; He et al., 2021). Nevertheless, there was no study analyzing the

function of miR-541-3p in cervical cancer. The function of miR-541-3p in cervical cancer and its functional correlation with circ_0085616 were therefore explored.

It is widely accepted that miRNAs can interact with target messenger RNAs (mRNAs) at the 3' untranslated region (3'UTR) to modulate gene expression in human cancers (Pu et al., 2019). Through bioinformatics prediction, ADP ribosylation factor like GTPase 2 (ARL2) was one of the possible targets of miR-541-3p. ARL2 is a member of the small G-protein family (Wang et al., 2018). Small G-proteins are crucial regulatory factors in multiple pathways (Matozaki et al., 2000). In addition, ARL2 is reported to contribute to cervical cancer progression (Chen et al., 2020). In the present study, we discussed the interplay among circ_0085616, miR-541-3p, and ARL2.

In our study, the function of circ_0085616 in cervical cancer cells was analyzed. Then, its potential working mechanism related to miR-541-3p and ARL2 was explored.

Materials and methods

Clinical samples

Thirty-one patients diagnosed with cervical cancer at First Affiliated Hospital of Jinzhou Medical University were recruited in the clinical study. All patients had signed the written informed consent to donate their tumor tissues for medical study. All patients have not received chemotherapy, radiotherapy, or immunotherapy. In addition to the cervical cancer tissue specimens (n=31), the corresponding adjacent normal tissue specimens (n=31) were harvested as the normal controls. These excised tissues were stored in an ultra-low temperature refrigerator at -80°C. This study was approved by the Ethical Committee of First Affiliated Hospital of Jinzhou Medical University.

Cell culture

Human cervical cancer cell lines (SiHa and C33A), normal ectocervical cell line (ECT1/E6E7), and human umbilical vein endothelial cells (HUVEC) were obtained from Bena Culture Collection (Beijing, China). All cells were maintained in Dulbecco's modified eagle medium (DMEM; Gibco, Carlsbad, CA, USA) added with 10% fetal bovine serum (FBS; Gibco) and 1% streptomycin-penicillin solution (Gibco) at 37°C with 5% CO_2.

Subcellular localization

The extraction of cytoplasmic and nuclear RNAs was conducted using the PARIS^{TM} Kit Protein and RNA Isolation system (Thermo Fisher Scientific, Waltham, MA, USA).

Reverse transcription-quantitative polymerase chain reaction (RT-qPCR)

RNAiso Plus (Takara, Beijing, China) was utilized during RNA isolation. The complementary DNA (cDNA) was acquired via the commercial First-Strand cDNA Synthesis kit (for circRNAs and mRNAs; Thermo Fisher Scientific) and miRNA stem-loop primer (for miRNAs; RiboBio, Guangzhou, China). Then, qPCR reaction was conducted on the Applied Biosystems 7500 Fast Real-Time PCR System (Applied Biosystems, Foster City, CA, USA) using SYBR Premix Ex Taq (Takara). All primers are given in Table 1. U6 and β-Actin were used as the internal references for miRNAs and circRNAs/mRNAs, respectively. The $2^{-\Delta\Delta CT}$ method was utilized to analyze the relative gene expression.

Cell transfection

Small interfering RNA against the junction sites of circ_0085616 (si-circ_0085616), negative control of siRNA (si-NC), short hairpin RNA against the junction sites of circ_0085616 (sh-circ_00856161), sh-NC, circ_0085616 overexpression plasmid (oe-circ_0085616), empty pLO-ciR vector (vector), miR-541-3p mimic, miR-NC mimic, miR-541-3p inhibitor (anti-miR-541-3p), anti-miR-NC, ARL2 overexpression plasmid in pcDNA vector (pcDNA-ARL2), and pcDNA-NC were synthesized or constructed by GenePharma (Shanghai, China).

Colony formation assay

To analyze the radio-resistance of cervical cancer cells, cells were seeded onto 6 cm culture plate (n=3 for each dose). Then, cells were irradiated with 0, 2, 4, 6, or 8 Gy, and incubated for 12 d. The colonies were washed with PBS, immobilized with 4% paraformaldehyde (Sangon Biotech, Shanghai, China) for 15 min, and stained with 0.1% crystal violet (Sangon Biotech) for 15

Table 1. Primer sequences in RT-qPCR assay.

Gene	Direction	Sequence
circ_0085616	forward	5'-GACTACAACTCGCCCACCAC-3'
	reverse	5'-ACCATGCCTCAGTGAAAACC-3'
miR-541-3p	forward	5'-TCGGCAGGTGGTGGGCACAGAA-3'
	reverse	5'-CAGTGCAGGGTCCGAGGTAT-3'
ARL2	forward	5'-GGTGGAGGAGGTCCTGGAG-3'
	reverse	5'-GTGAAGGTTGAGGGACCTGG-3'
β-actin	forward	5'-CTCGCCTTTGCCGATCC-3'
	reverse	5'-TCTCCATGTCGTCCCAGTTG-3'
U6	forward	5'-CTCGCTTCGGCAGCACA-3'
	reverse	5'-AACGCTTCACGAATTTGCGT-3'
GAPDH	forward	5'-TATGATGACATCAAGAAGGTGGT-3'
	reverse	5'-TGTAGCCAAATTCGTTGTCATAC-3'

min. The number of colonies (>50 cells) was counted under an optical microscope (Olympus, Tokyo, Japan).

To analyze the proliferation ability of cervical cancer cells, cells were plated onto 12-well plates and incubated for 12 d. The colony number (>50 cells) was analyzed under an optical microscope (Olympus).

5-ethynyl-2'-deoxyuridine (EdU) assay

Cervical cancer cells were mixed with 50 μM EdU reagent of Cell-Light™ EdU Apollo®567 *In Vitro* Imaging Kit (RiboBio) for 2h. 4, 6-diamino-2-phenylindole dye liquor (DAPI; Sigma-Aldrich, St. Louis, MO, USA) was utilized to mark cell nucleus. Cell images were captured by a fluorescence microscope (Olympus).

Flow cytometry (FCM) analysis

Cells were collected with EDTA-free trypsin (Thermo Fisher Scientific) and suspended in PBS buffer after 72 h-transfection. The dye solution (HEPES buffer: Annexin-V-FITC: PI=50:1:2; Sigma-Aldrich) was prepared, and cells were incubated with 100 μL of dye solution. The apoptotic cells were identified by flow cytometer (BD Biosciences, Franklin Lakes, NJ, USA).

Tube formation assay

HUVECs were cultured with the culture supernatant of transfected cervical cancer cells in 96-well plates covered with Matrigel (BD Biosciences). After incubation for 10h, the relative tube formation rate was analyzed by counting the average number of branches of each node.

Transwell assays

Transfected cervical cancer cells were suspended in culture media without serum. Then, cell suspension ($2x10^4$ cells for transwell migration assay, $9x10^4$ cells for transwell invasion assay) was added to the top cambers with (invasion assay) or without (migration assay) Matrigel (BD Biosciences). The culture media added with 10% FBS was pipetted to the bottom chambers. The metastatic cells were stained with 0.5% crystal violet (Sangon Biotech), photographed at 100x, and counted.

Western blot assay

Tissues and cells were lysed with radio-immunoprecipitation assay (RIPA) buffer (Beyotime, Jiangsu, China). Protein specimens were loaded onto 10% sodium dodecyl sulfate-polyacrylamide gel electrophoresis and shifted to a polyvinylidene difluoride membrane (Millipore, Billerica, MA, USA). The membrane was incubated with PBST for 1h containing 5% non-fat milk. Then, the membrane was incubated with the primary antibodies against matrix metallopeptidase 2 (MMP-2; 1:1000, ab181286, Abcam, Cambridge, MA, USA), MMP-9 (1:1000, ab38898, Abcam), ARL2 (1:10000, ab183510, Abcam), and β-Actin (1:1000, ab8227, Abcam) overnight at 4°C. Subsequently, secondary antibody (1:50,000, ab205718, Abcam) was mixed with the membrane for 1h. The immunoblots were analyzed via the enhanced chemiluminescence (ECL) kit (Pierce, Waltham, MA, USA).

Bioinformatics analysis

The interacted miRNAs of circ_0085616 and the interacted mRNAs of miR-541-3p were sought by Starbase database.

Dual-luciferase reporter assay

The wild-type (WT) fragment of circ_0085616 or the 3'UTR of ARL2 was amplified by PCR, and the mutant type (MUT) fragment of circ_0085616 or the 3'UTR of ARL2 was synthesized via site-directed mutation. The amplified PCR products were constructed into pmirGLO plasmid (Promega, Madison, WI, USA) to generate WT/MUT-circ_0085616 and WT/MUT-ARL2 3'UTR. The luciferase activities were determined via the commercial Dual-Luciferase® Reporter assay kits (Promega).

Xenograft mouse model

Ten BALB/c female nude mice (5-week-old) were purchased from Vital River Laboratory Animal Technology (Beijing, China). A total of $2x10^6$ SiHa cells stably expressing sh-NC or sh-circ_0085616 were injected into the nude mice (n=5 in each group). The volume of xenograft tumors was analyzed using a digital caliper every week as length×width^2×0.5. After injection for 4 weeks, the nude mice were killed via the CO_2 asphyxia method, and tumor weight was recorded. The ARL2 and Ki67 positive cells (brown nucleus) were measured by immunohistochemistry (IHC) assay. Briefly, paraffin-embedded fresh tumor tissues were cut into slices 4 μm thick. After antigen recovery in a citrate buffer, the sections were incubated with anti-Ki67 (1:200, ab15580, Abcam) or anti-ARL2 (1:500, ab183510, Abcam) and then incubated with HRP conjugated Goat anti-Rabbit IgG (1:10000, ab205718, Abcam). After staining by DAB reagents and hematoxylin, the sections were analyzed to observe the staining results under a microscope. The number of ARL2 and Ki67 positive cells was recorded as brown nuclei. Animal experiment was approved by the Animal Ethical Committee of First Affiliated Hospital of Jinzhou Medical University.

Statistical analysis

The differences between groups were evaluated by Graphpad Prism 7 (GraphPad, La Jolla, CA, USA). Data were expressed in the form of mean ± standard deviation. The differences in two groups or multiple groups were analyzed by Student's t-test or one-way analysis of variance (ANOVA) followed by Tukey's test. $P<0.05$ indicated the significant differences.

Results

Circ_0085616 level is increased in cervical cancer tissues and cell lines

We analyzed the expression of circ_0085616 in cervical cancer tissues and cell lines. RT-qPCR assay presented that circ_0085616 expression was markedly elevated in cervical cancer tissues and cell lines compared with paired normal tissues and Ect1/E6E7 cell line (Fig. 1A,B). We then analyzed the subcellular localization of circ_0085616 in cervical cancer cells with GAPDH or U6 as cytoplasmic or nuclear marker. The results displayed that circ_0085616 was majorly distributed in the cytoplasm of cervical cancer cells (Fig. 1C), indicating that circ_0085616 might serve as a miRNA sponge. Abnormal up-regulation of circ_0085616 might imply its important regulatory role in cervical cancer.

Circ_0085616 silencing restrains the radio-resistance and malignant behaviors of cervical cancer cells

To explore the role of circ_0085616, loss-of-function experiments using si-circ_0085616 were conducted. RT-qPCR assay showed that si-circ_0085616 was effective in silencing circ_0085616 in both cervical cancer cell lines (Fig. 2A). Colony formation assay was conducted to analyze the effect of circ_0085616 knockdown on the radio-resistance of cervical cancer cells. The survival fractions in both si-NC and si-circ_0085616 groups were decreased upon irradiation in a dose-dependent manner (Fig. 2B). Furthermore, it was observed that circ_0085616 silencing elevated the radio-sensitivity of cervical cancer cells (Fig. 2B). Colony formation assay was also performed to analyze the proliferation ability of cervical cancer cells along with EdU assay. Circ_0085616 knockdown reduced the number of colonies and the percentage of EdU^+ cells (Fig. 2C,D), suggesting that circ_0085616 knockdown restrained the proliferation of cervical cancer cells. FCM analysis displayed that the apoptosis rate was significantly elevated in circ_0085616-silenced group compared with si-NC group (Fig. 2E). Circ_0085616 interference suppressed the angiogenesis ability of cervical cancer cells (Fig. 3A), evidenced by the reduced number of branches of each node. Circ_0085616 interference decreased the numbers of migrated and invaded cells (Fig. 3B,C), suggesting that circ_0085616 knockdown suppressed the motility of cervical cancer cells. Two cell motility-associated proteins (MMP-2 and MMP-9) were detected by Western blot assay. The results presented that circ_0085616 silencing reduced the levels of MMP-2 and MMP-9 (Fig. 3D,E). Taken together, circ_0085616 knockdown suppressed the radio-resistance, proliferation, tube formation, migration, and invasion and triggered the apoptosis of cervical cancer cells.

Circ_0085616 acts as a molecular sponge for miR-541-3p

To investigate the working mechanism of circ_0085616, we predicted the interacted miRNAs of circ_0085616 using Starbase bioinformatics database. The complementary sites between circ_0085616 and miR-541-3p are shown in Fig. 4A. RT-qPCR assay verified that the overexpression efficiency of miR-541-3p mimic was high in cervical cancer cells (Fig. 4B). Dual-luciferase reporter assay was implemented to verify the target relationship between circ_0085616 and miR-541-3p. The luciferase activity was notably decreased in WT-circ_0085616 and miR-541-3p mimic co-transfected group compared with WT-circ_0085616 and miR-NC mimic group (Fig. 4C). Meanwhile, the transfection of miR-NC mimic or miR-541-3p mimic caused similar luciferase activity in MUT-circ_0085616 group (Fig. 4C), indicating that circ_0085616 interacted

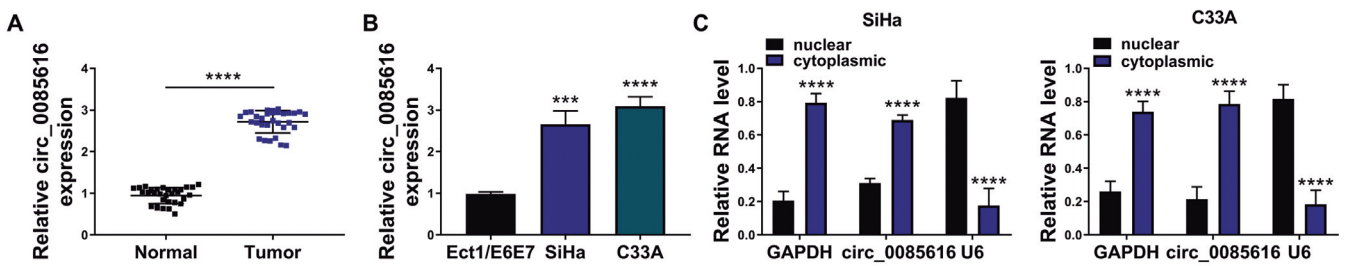

Fig. 1. Circ_0085616 level is increased in cervical cancer tissues and cell lines. **A.** We collected 31 pairs of cervical tissues and adjacent normal tissues, and RT-qPCR was performed to analyze the expression of circ_0085616 in tumor tissues and para-cancer tissues. **B.** The level of circ_0085616 was determined in cervical cancer cell lines (SiHa and C33A) and Ect1/E6E7 by RT-qPCR. **C.** The subcellular localization of circ_0085616 in SiHa and C33A cells was analyzed using commercial kit. ***$P<0.001$, ****$P<0.0001$.

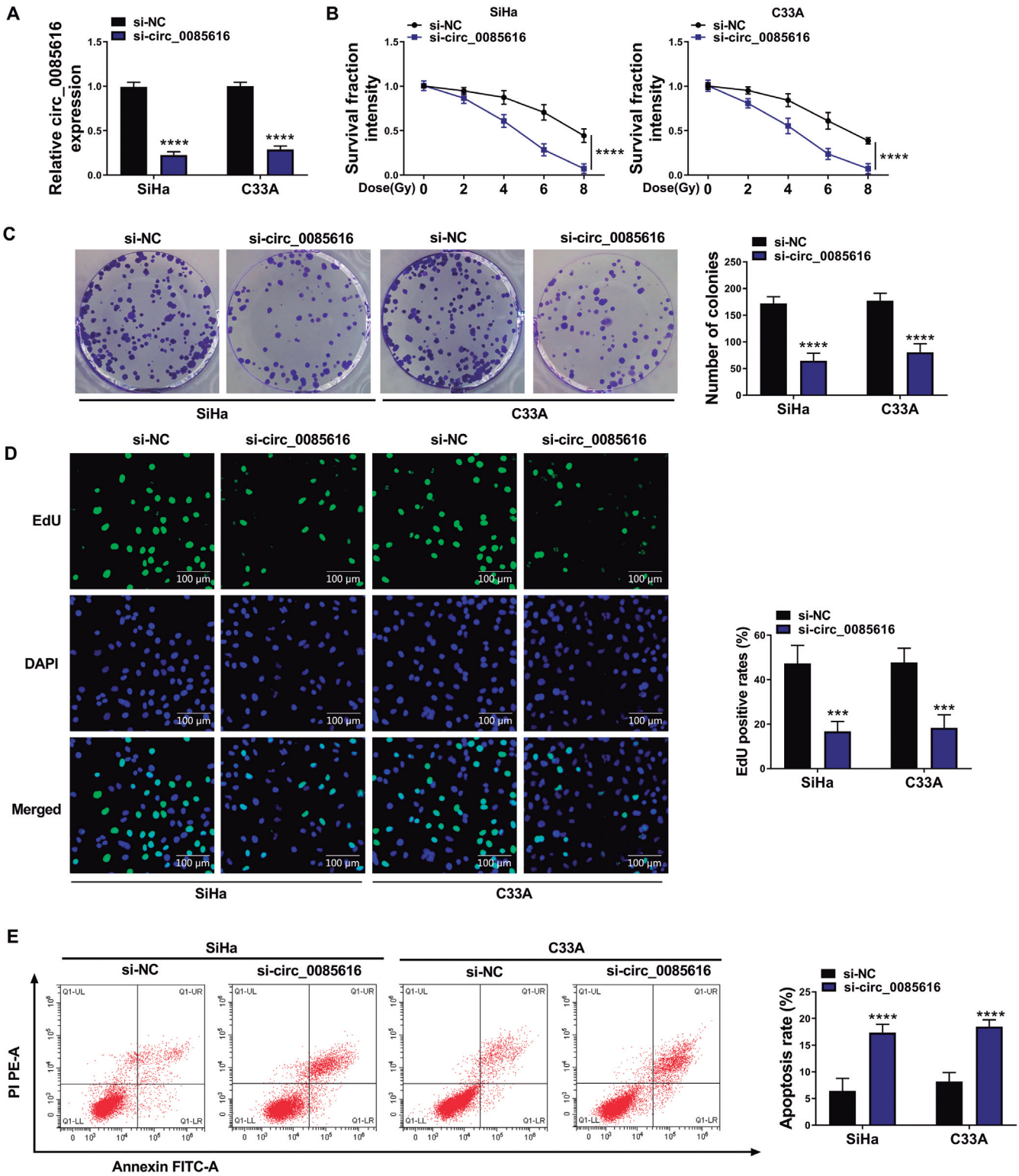

Fig. 2. Circ_0085616 silencing restrains the radio-resistance and malignant behaviors of cervical cancer cells. SiHa and C33A cells were transfected with si-NC or si-circ_0085616. **A.** The efficiency of si-circ_0085616 in down-regulating circ_0085616 level in cervical cancer cells was assessed by RT-qPCR. **B.** Colony formation assay was performed to analyze the radio-resistance of transfected cervical cancer cells. **C, D.** Cell proliferation ability was analyzed by colony formation assay and EdU assay. **E.** FCM analysis was conducted to analyze the apoptosis rate of cervical cancer cells. ****P*<0.001, *****P*<0.0001.

with miR-541-3p via the predicted sites. High overexpression efficiency of circ_0085616 plasmid (oe-circ_0085616) in cervical cancer cells was verified by RT-qPCR assay (Fig. 4D). We analyzed the effects of circ_0085616 overexpression and knockdown on the level of miR-541-3p in cervical cancer cells. Circ_0085616 overexpression markedly reduced miR-541-3p level, while circ_0085616 silencing caused a notable up-regulation in the expression of miR-541-3p in cervical cancer cells (Fig. 4E), suggesting that circ_0085616 negatively regulated miR-541-3p level in cervical cancer cells. miR-541-3p level was reduced in cervical cancer tissues and cell lines compared with adjacent normal tissues and Ect1/E6E7 cell line (Fig. 4F,G). These results indicated that circ_0085616 negatively regulated miR-541-3p level by binding to it.

Circ_0085616 silencing inhibits the radio-resistance and malignant behaviors of cervical cancer cells partly by up-regulating miR-541-3p

To investigate whether the effects of circ_0085616 in cervical cancer cells were partly dependent on its regulation of miR-541-3p, we performed compensation experiments. SiHa and C33A cells were transfected with si-circ_0085616 alone or together with anti-miR-541-3p. Circ_0085616 silencing up-regulated miR-541-3p expression in cervical cancer cells, and this effect was partly counteracted by anti-miR-541-3p (Fig. 5A). The addition of anti-miR-541-3p partly rescued the radio-resistance of cervical cancer cells (Fig. 5B). Moreover, colony formation assay and EdU assay together demonstrated that circ_0085616 silencing-mediated suppressive effect on the proliferation of cervical cancer cells was reversed by anti-miR-541-3p (Fig. 5C,D). FCM analysis displayed that circ_0085616 interference-induced apoptosis of cervical cancer cells was diminished in si-circ_0085616 and anti-miR-541-3p co-transfected group (Fig. 5E). The introduction of anti-miR-541-3p also partly restored the angiogenesis, migration, and invasion abilities of cervical cancer cells (Fig. 6A-C). Western blot assay presented that the levels of MMP-2 and MMP-9 were partly recovered by the addition of anti-miR-541-3p (Fig. 6D). These results

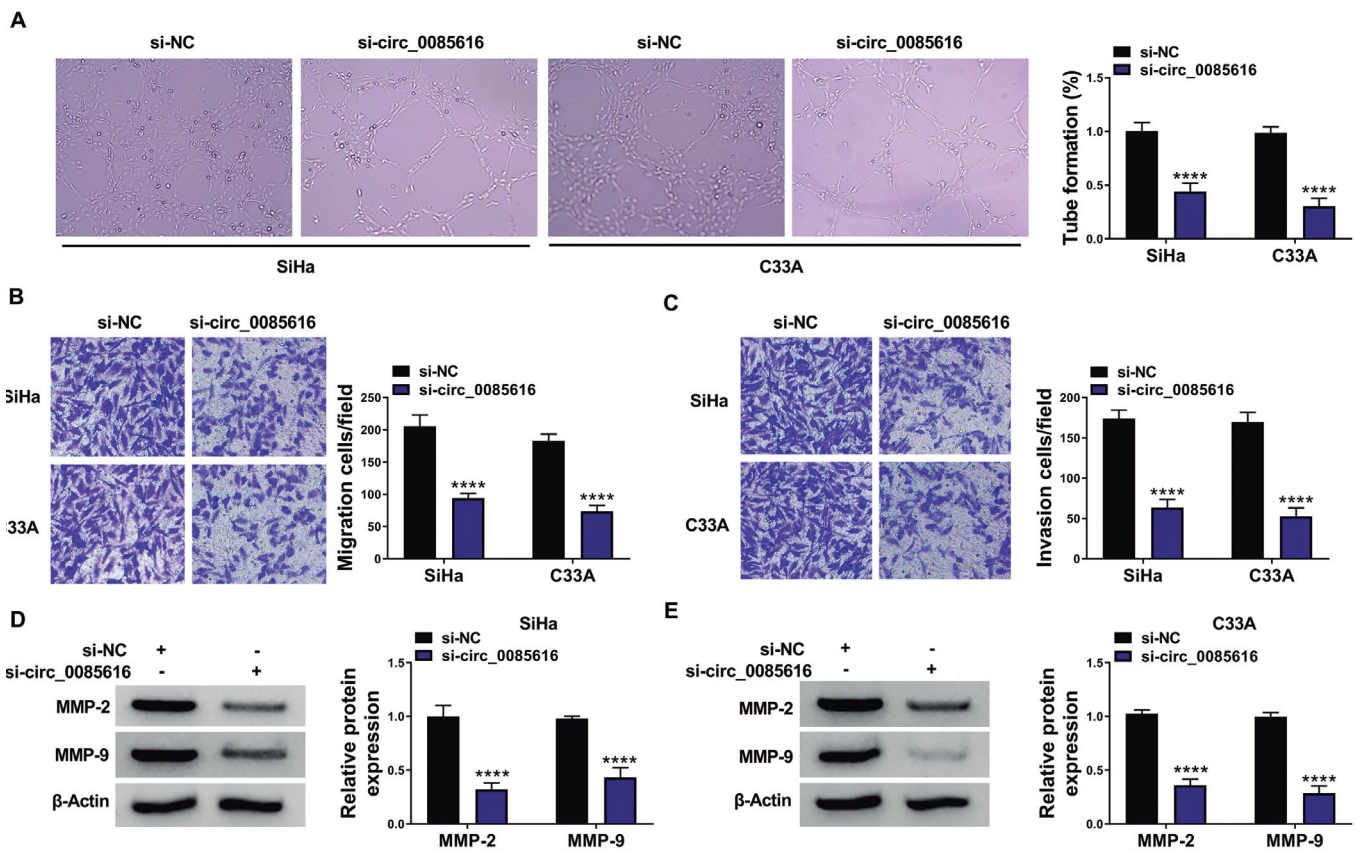

Fig. 3. Circ_0085616 silencing suppressed cervical cancer cell progression. SiHa and C33A cells were transfected with si-NC or si-circ_0085616. **A.** Tube formation assay was performed to analyze the angiogenesis ability of cervical cancer cells. **B, C.** Transwell assays were performed to analyze the migration and invasion abilities of cervical cancer cells. **D, E.** The protein levels of MMP-2 and MMP-9 were measured by Western blot assay. ****P<0.0001.

together suggested that circ_0085616 silencing-induced inhibitory effects on cervical cancer progression were partly based on the up-regulation of miR-541-3p.

miR-541-3p binds to the 3'UTR of ARL2

To better understand the molecular mechanism underlying circ_0085616/miR-541-3p axis in cervical cancer cells, the mRNA targets of miR-541-3p were predicted by Starbase bioinformatics database. The putative binding sequence between miR-541-3p and the 3'UTR of ARL2 is shown in Fig. 7A. SiHa and C33A cells were co-transfected with miR-NC mimic or miR-541-3p mimic and WT-ARL2 3'UTR or MUT-ARL2 3'UTR. In WT-ARL2 3'UTR group, transfection with miR-541-3p mimic rather than miR-NC mimic significantly reduced the luciferase activity (Fig. 7B). However, in MUT-ARL2 3'UTR group, luciferase activity was unchanged with the transfection of miR-NC mimic or miR-541-3p mimic (Fig. 7B), suggesting the direct interaction between miR-541-3p and ARL2 3'UTR via the putative sites. RT-qPCR presented that anti-miR-541-3p was effective in down-regulating miR-541-3p expression in cervical cancer cells (Fig. 7C). miR-541-3p silencing up-regulated the protein expression of ARL2, while miR-541-3p overexpression reduced ARL2 protein level in cervical cancer cells (Fig. 7D). Both the mRNA and protein expression of ARL2 were elevated in cervical cancer tissues compared with adjacent normal tissues (Fig. 7,F). The protein expression of ARL2 was markedly more up-regulated in cervical cancer cell lines than that in Ect1/E6E7 cell line

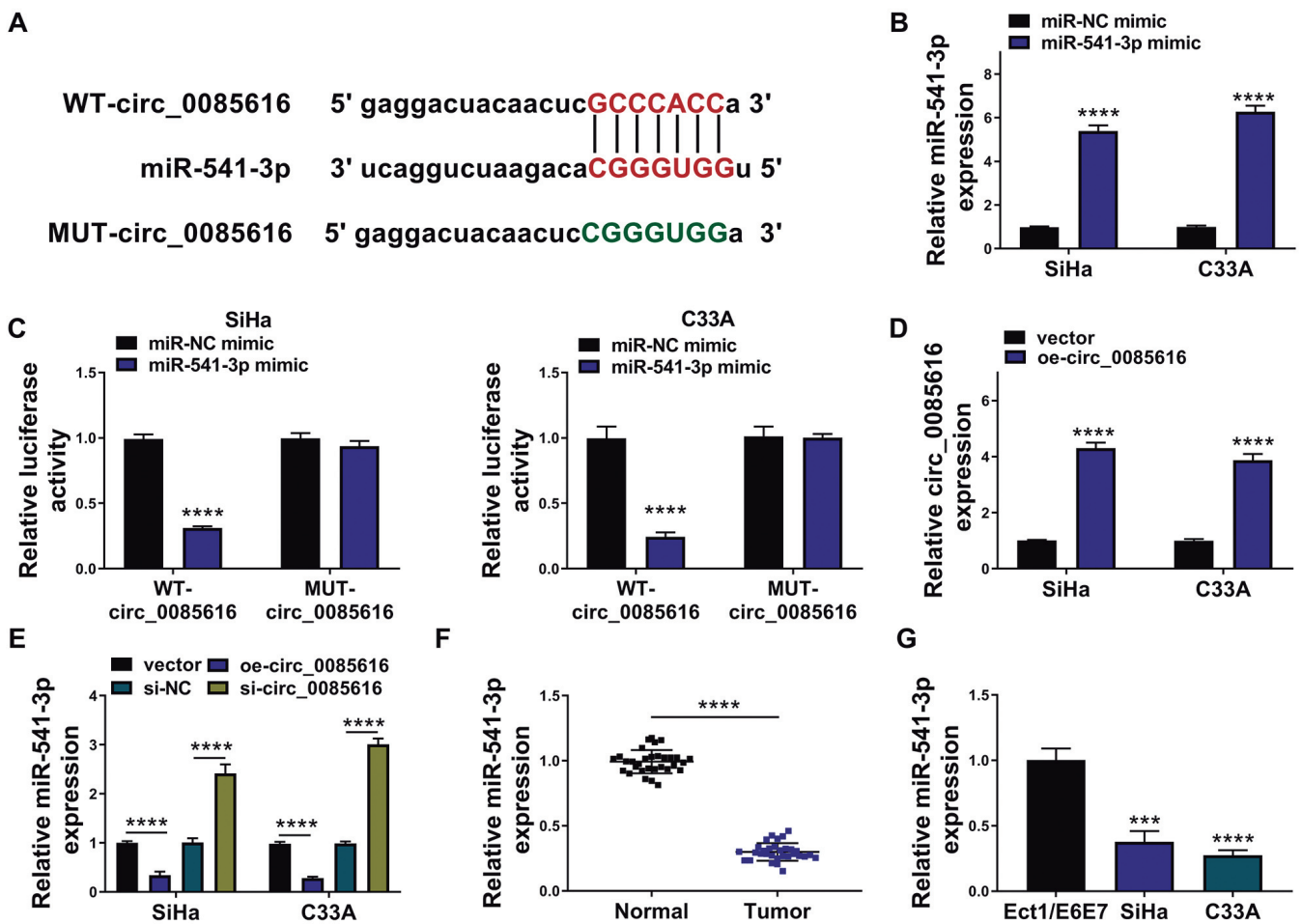

Fig. 4. Circ_0085616 acts as a molecular sponge for miR-541-3p. **A.** Starbase bioinformatics software predicted the binding sequence between circ_0085616 and miR-541-3p. **B.** RT-qPCR assay assessed the efficiency of miR-541-3p mimic in up-regulating miR-541-3p expression in cervical cancer cells. **C.** The interaction between circ_0085616 and miR-541-3p was verified by dual-luciferase reporter assay. **D.** The overexpression efficiency of circ_0085616 overexpression plasmid (oe-circ_0085616) was analyzed by RT-qPCR. **E.** The regulatory relationship between circ_0085616 and miR-541-3p was analyzed. RT-qPCR was employed to detect the expression of miR-541-3p in cervical cancer cells transfected with vector, oe-circ_0085616, si-NC, or si-circ_0085616. **F.** RT-qPCR was conducted to measure miR-541-3p expression in 31 pairs of cervical tissues and adjacent normal tissues. **G.** The level of miR-541-3p was examined in cervical cancer cells and Ect1/E6E7 by RT-qPCR. ***P<0.001, ****P<0.0001.

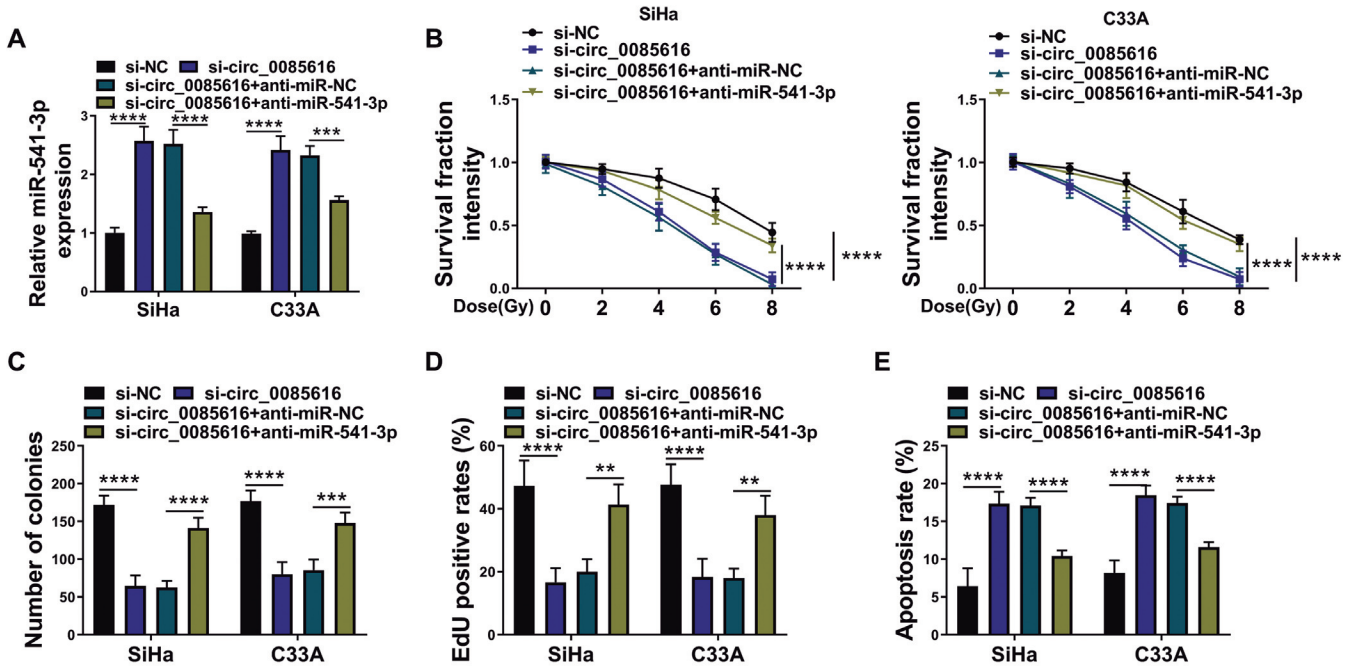

Fig. 5. Circ_0085616 silencing inhibits the radio-resistance and malignant behaviors of cervical cancer cells partly by up-regulating miR-541-3p. SiHa and C33A cells were transfected with si-circ_0085616 alone or together with anti-miR-541-3p. **A.** RT-qPCR was implemented to analyze the level of miR-541-3p in transfected cervical cancer cells. **B.** Colony formation assay was employed to assess the radio-resistance of cervical cancer cells. **C, D.** Cell proliferation capacity was assessed by colony formation assay and EdU assay. **E.** The apoptosis rate of cervical cancer cells was measured by FCM analysis. **F.** The angiogenesis ability of cervical cancer cells was evaluated by tube formation assay. **G, H.** The migration and invasion abilities of cervical cancer cells were assessed by transwell migration and invasion assays. **I.** The protein expression of MMP-2 and MMP-9 was determined by Western blot assay. ***P*<0.01, ****P*<0.001, *****P*<0.0001.

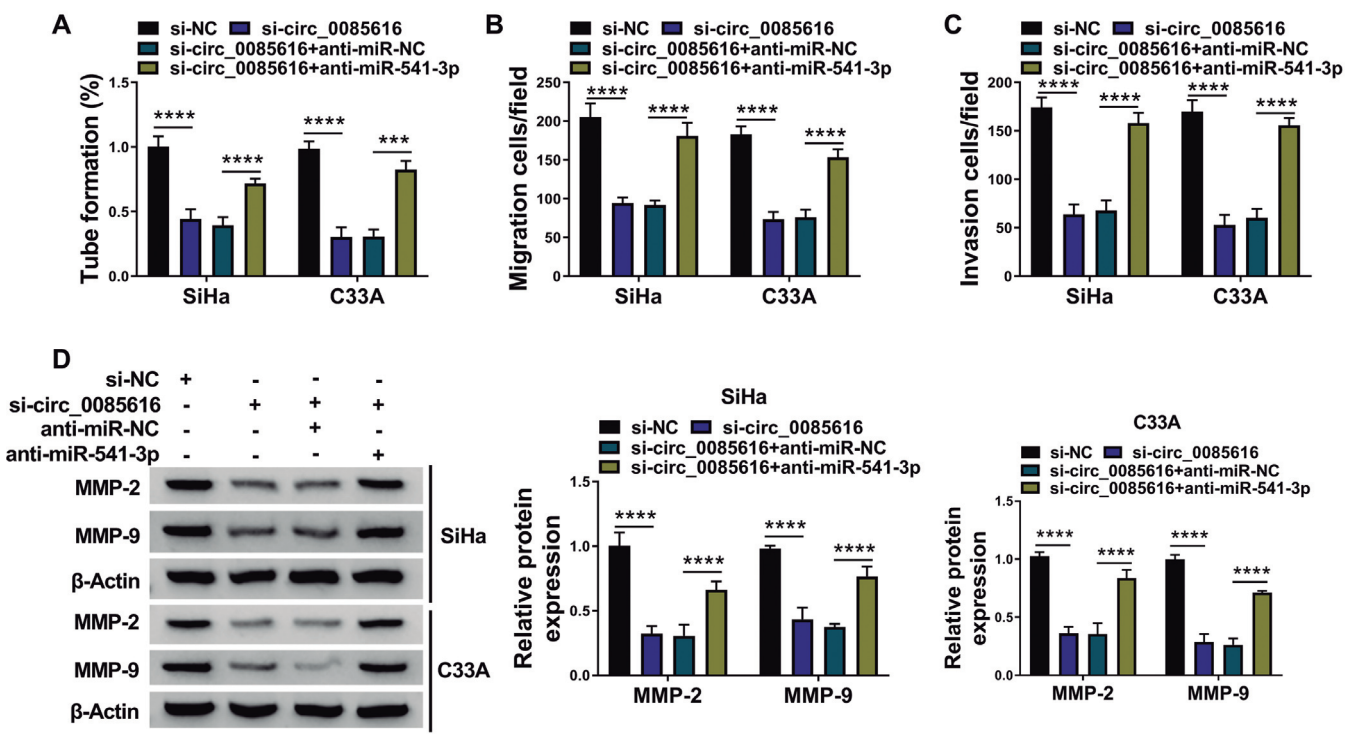

Fig. 6. Circ_0085616 silencing miR-541-3p to regulate cervical cancer cell progression. SiHa and C33A cells were transfected with si-circ_0085616 alone or together with anti-miR-541-3p. **A.** The angiogenesis ability of cervical cancer cells was evaluated by tube formation assay. **B, C.** The migration and invasion abilities of cervical cancer cells were assessed by transwell migration and invasion assays. **D.** The protein expression of MMP-2 and MMP-9 was determined by Western blot assay. ****P*<0.001, *****P*<0.0001.

(Fig. 7G). These findings together demonstrated that miR-541-3p directly interacted with the 3'UTR of ARL2.

The biological effects induced by miR-541-3p overexpression are partly reversed by the introduction of pcDNA-ARL2 in cervical cancer cells

To explore whether the effects of miR-541-3p in cervical cancer cells were partly based on the regulation of ARL2, rescue experiments were carried out. Cervical cancer cells were transfected with miR-541-3p mimic alone or together with pcDNA-ARL2. miR-541-3p overexpression reduced the protein level of ARL2, and the protein level of ARL2 was largely restored by the addition of pcDNA-ARL2 (Fig. 8A). miR-541-3p overexpression suppressed the radio-resistance of cervical cancer cells, and the radio-resistance of cervical cancer cells was partly restored by pcDNA-ARL2 (Fig. 8B). miR-541-3p overexpression inhibited the proliferation ability of cervical cancer cells, and the introduction of ARL2 plasmid partly recovered the proliferation ability (Fig. 8C,D). Cell apoptosis was triggered by miR-541-3p overexpression, and the addition of pcDNA-ARL2 restrained miR-541-3p-induced apoptosis (Fig. 8E). miR-541-3p overexpression suppressed the angiogenesis, migration, and invasion abilities of cervical cancer cells, and these suppressive effects were largely counteracted by pcDNA-ARL2 (Fig. 9A-C). The levels of MMP-2 and MMP-9 were decreased by miR-541-3p overexpression, which were partly rescued by the addition of pcDNA-ARL2 (Fig. 9D-F). Taken together, miR-541-3p overexpression suppressed the radio-resistance and progression of

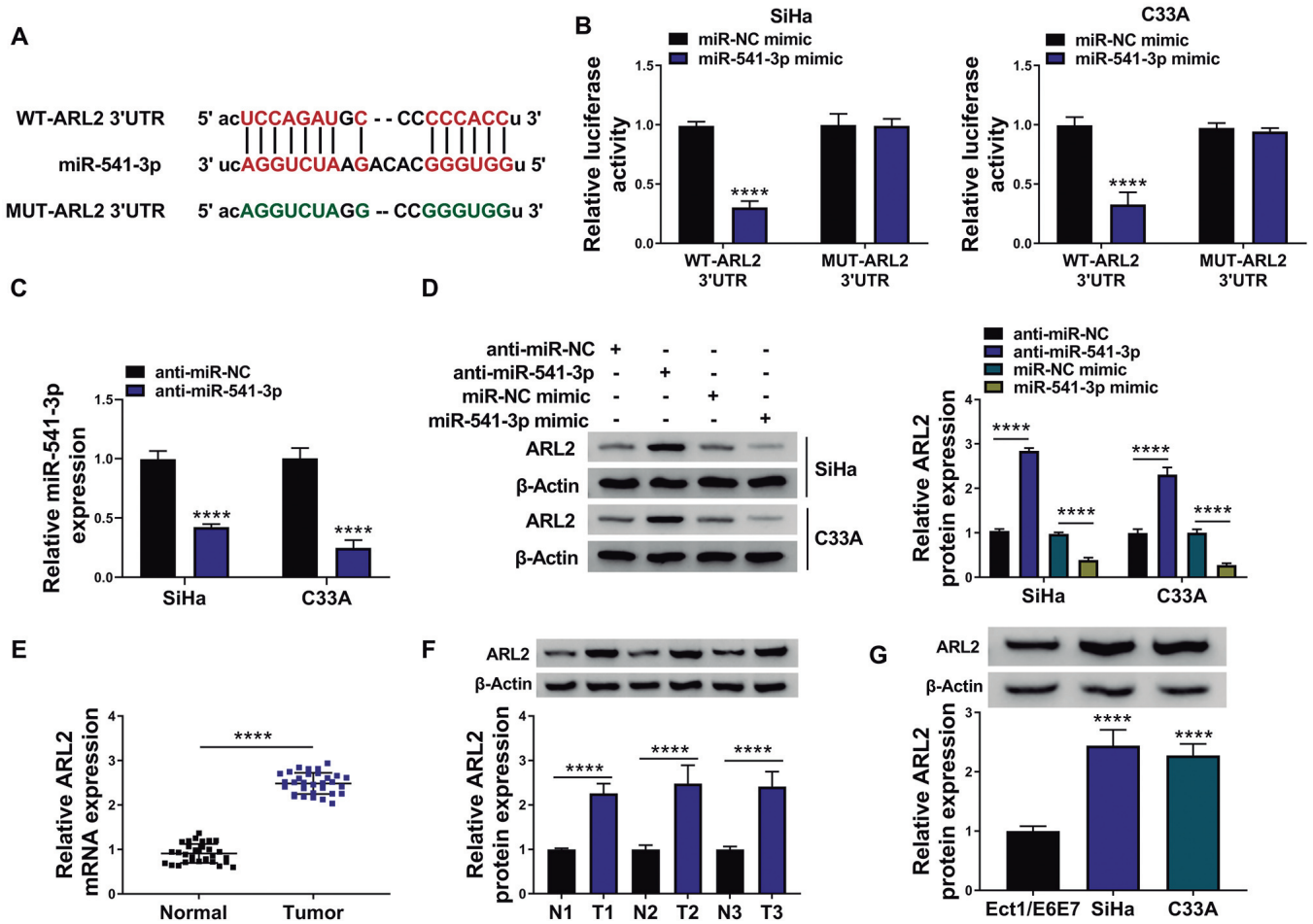

Fig. 7. miR-541-3p binds to the 3'UTR of ARL2. **A.** The potential binding sites between ARL2 3'UTR and miR-541-3p were predicted by Starbase bioinformatics database. **B.** The associated relationship between miR-541-3p and ARL2 was confirmed by dual-luciferase reporter assay. **C.** The transfection efficiency of anti-miR-541-3p was examined by RT-qPCR. **D.** Western blot assay was conducted to measure the protein level of ARL2 in cervical cancer cells transfected with anti-miR-NC, anti-miR-541-3p, miR-NC mimic, or miR-541-3p mimic. **E, F.** RT-qPCR and Western blot assay were performed to detect the mRNA and protein expression of ARL2 in cervical cancer tissues and para-cancer tissues. **G.** Western blot assay was employed to determine the protein expression of ARL2 in cervical cancer cell lines and Ect1/E6E7 cell line. *****P*<0.0001.

cervical cancer partly by down-regulating ARL2.

ARL2 is regulated by circ_0085616/miR-541-3p signaling in cervical cancer cells

Circ_0085616 silencing reduced the protein expression of ARL2, and the addition of anti-miR-541-3p partly rescued the level of ARL2 in cervical cancer cells (Fig. 10A-C). Circ_0085616 overexpression up-regulated the protein level of ARL2, and ARL2 protein level was reduced in oe-circ_0085616 and miR-541-3p mimic co-transfected group (Fig. 10D-F). These results demonstrated that circ_0085616 positively regulated ARL2 expression by absorbing miR-541-3p in cervical cancer cells.

Circ_0085616 silencing suppresses tumor growth in vivo

A xenograft mouse model was established to analyze the role of circ_0085616 *in vivo*. The nude mice were subcutaneously injected with SiHa cells stably transfected with sh-NC (n=5) or sh-circ_0085616 (n=5). It was found that xenograft tumors derived from SiHa cells stably transfected with sh-circ_0085616 were

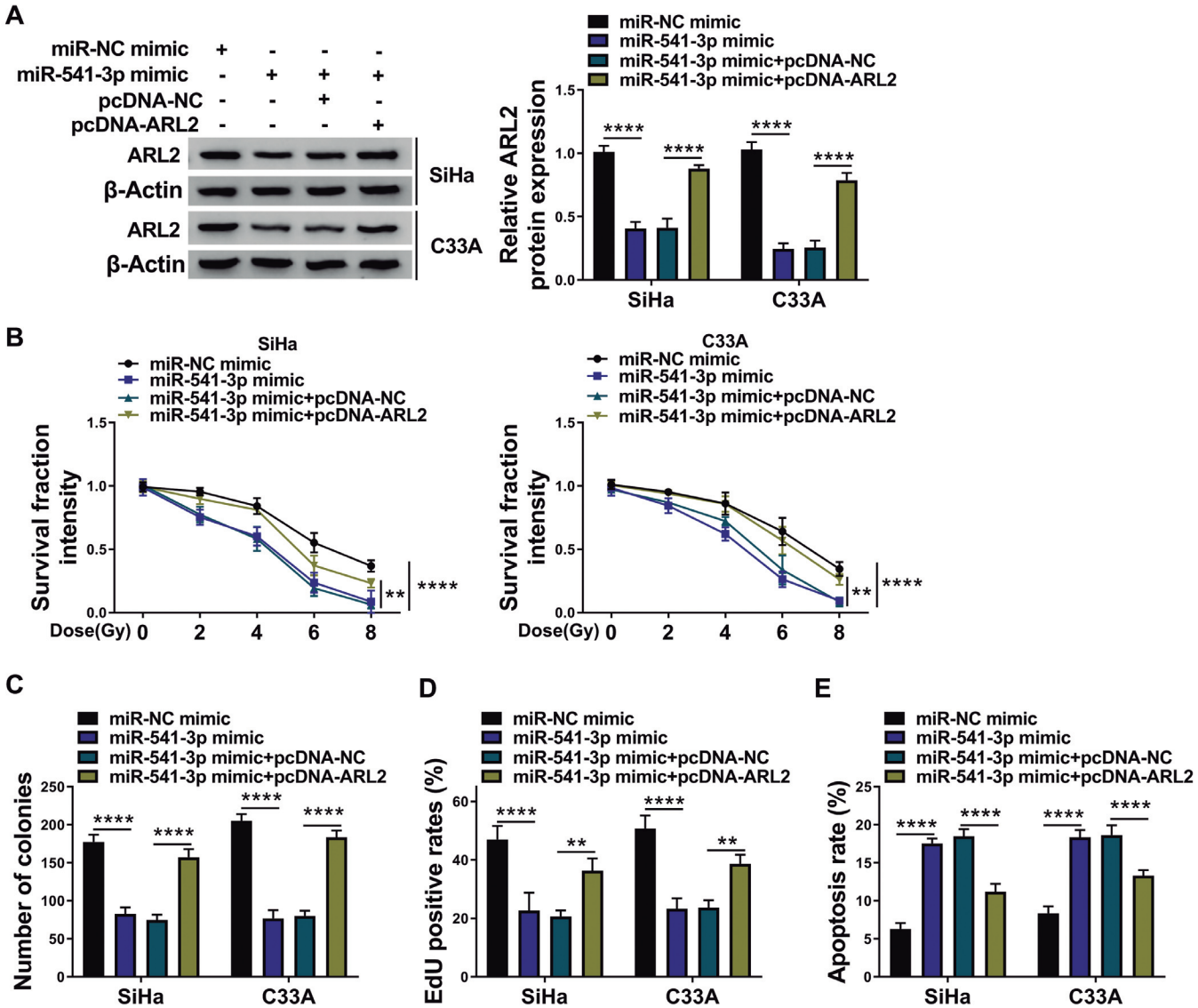

Fig. 8. The biological effects induced by miR-541-3p overexpression are partly reversed by the introduction of pcDNA-ARL2 in cervical cancer cells. SiHa and C33A cells were transfected with miR-541-3p mimic alone or together with pcDNA-ARL2. **A.** The protein level of ARL2 was examined by Western blot assay. **B.** The radio-resistance of cervical cancer cells was analyzed by colony formation assay. **C.** Colony formation assay was performed to measure the number of colonies to assess cell proliferation ability. **D.** EdU assay was conducted to detect the percentage of EdU$^+$ cells to assess cell proliferation ability. **E.** The apoptosis rate of cervical cancer cells was determined by FCM analysis. $^{**}P<0.01$, $^{***}P<0.001$, $^{****}P<0.0001$.

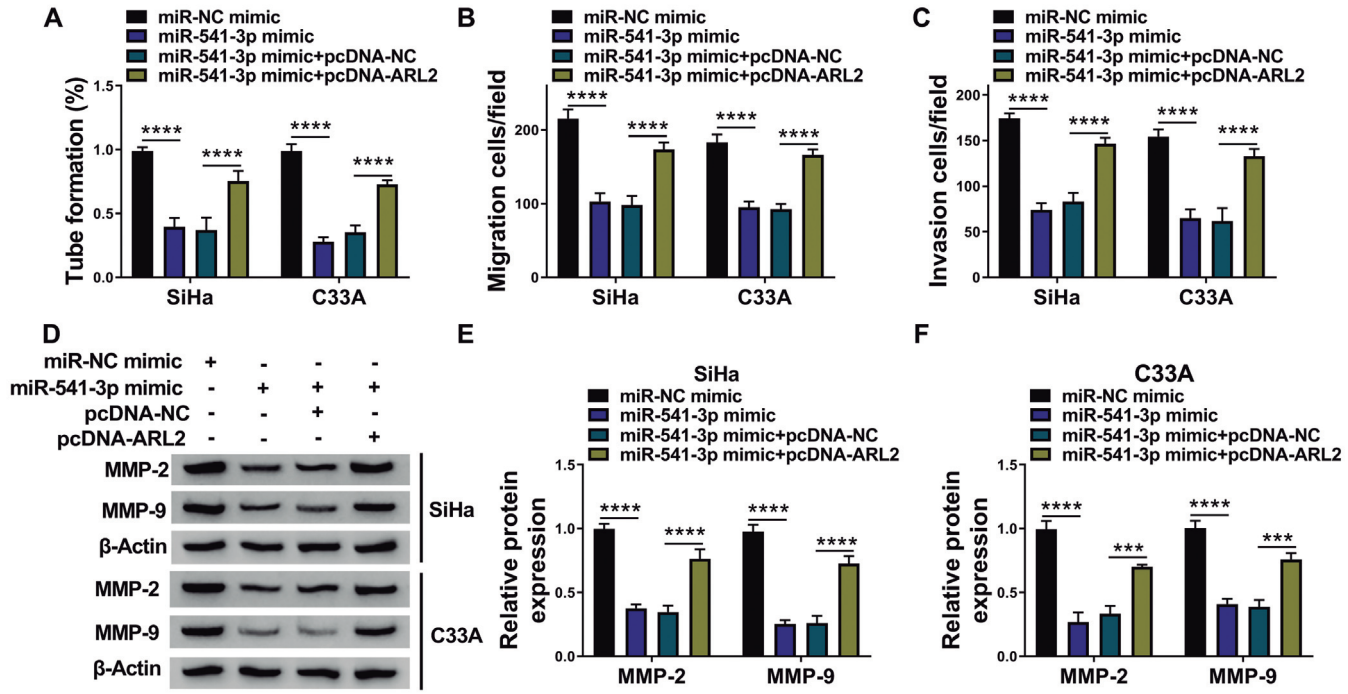

Fig. 9. MiR-541-3p and pcDNA-ARL2 overexpression regulated cervical cancer cell progression. SiHa and C33A cells were transfected with miR-541-3p mimic alone or together with pcDNA-ARL2. **A.** The angiogenesis ability of cervical cancer cells was examined by tube formation assay. **B, C.** Transwell migration and invasion assays were conducted to analyze the migration and invasion abilities of transfected cervical cancer cells. **D-F.** The protein expression of MMP-2 and MMP-9 was examined by Western blot assay. ****P*<0.001, *****P*<0.0001.

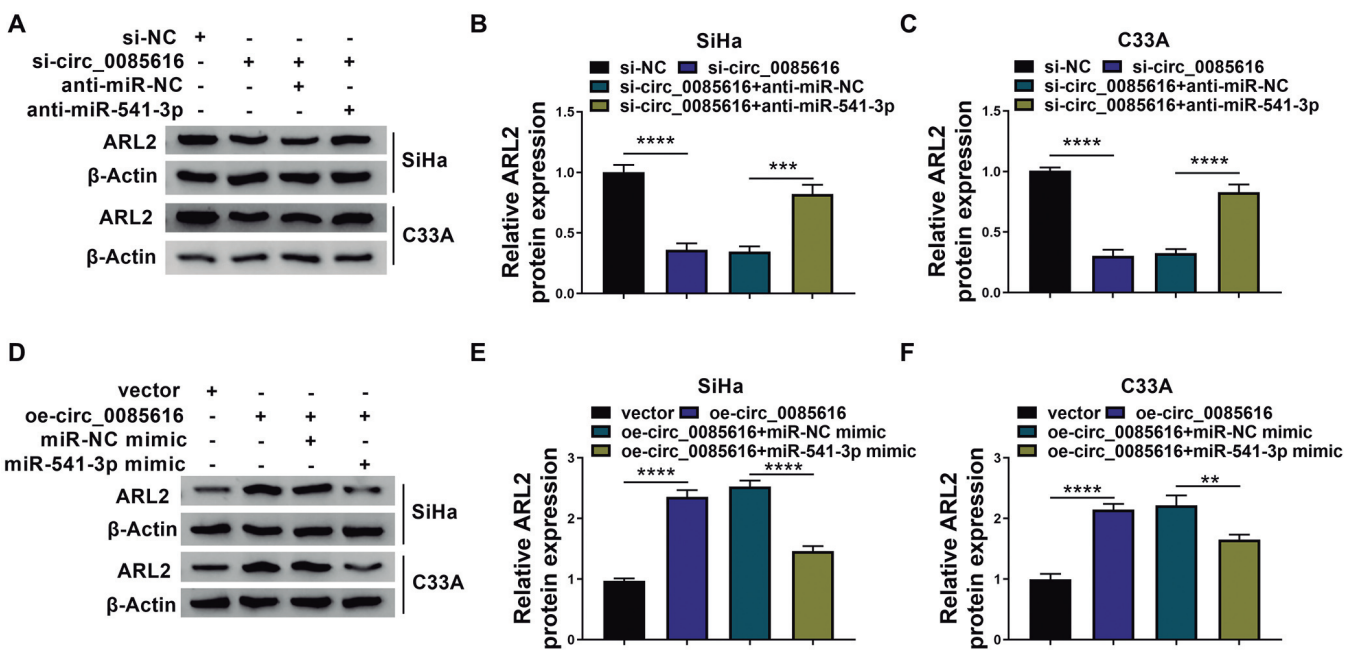

Fig. 10. ARL2 is regulated by circ_0085616/miR-541-3p signaling in cervical cancer cells. **A-C.** The protein level of ARL2 was determined in cervical cancer cells transfected with si-circ_0085616 alone or together with anti-miR-541-3p by Western blot assay. **D-F.** Western blot assay was employed to detect the protein expression of ARL2 in cervical cancer cells transfected with oe-circ_0085616 alone or together with miR-541-3p mimic. ***P*<0.01, ****P*<0.001, *****P*<0.0001.

smaller and lighter than that from SiHa cells stably transfected with sh-NC (Fig. 11A,B), suggesting that circ_0085616 silencing suppressed tumor growth *in vivo*. The expression of circ_0085616/miR-541-3p/ARL2 axis was determined in dissected tumor tissues. The expression of circ_0085616 and ARL2 protein was markedly reduced in circ_0085616-silenced tumor tissues, while circ_0085616 silencing up-regulated miR-541-3p expression in tumor tissues (Fig. 11C-E). The protein levels of ARL2 and Ki67 in tumor tissues were measured by IHC assay. The densities of ARL2 and Ki67 staining were lower in sh-circ_0085616 group than that in sh-NC group (Fig. 11F). These results demonstrated that circ_0085616 knockdown inhibited tumor growth *in vivo* partly by targeting the miR-541-3p/ARL2 axis.

Discussion

Identifying novel effective diagnostic and therapeutic targets is essential for cervical cancer treatment. We focused on a poorly studied circRNA, circ_0085616, in cervical cancer. CircRNAs are products of non-classical back-splicing of pre-mRNAs, and are circular single-stranded RNA molecules without 5' or 3' end (Chen and Yang, 2015). CircRNAs are ideal biomarkers for human diseases due to their several biological properties including the tissue-specific expression pattern, high stability, and resistance to exonuclease (Meng et al., 2017; Gao et al., 2018).

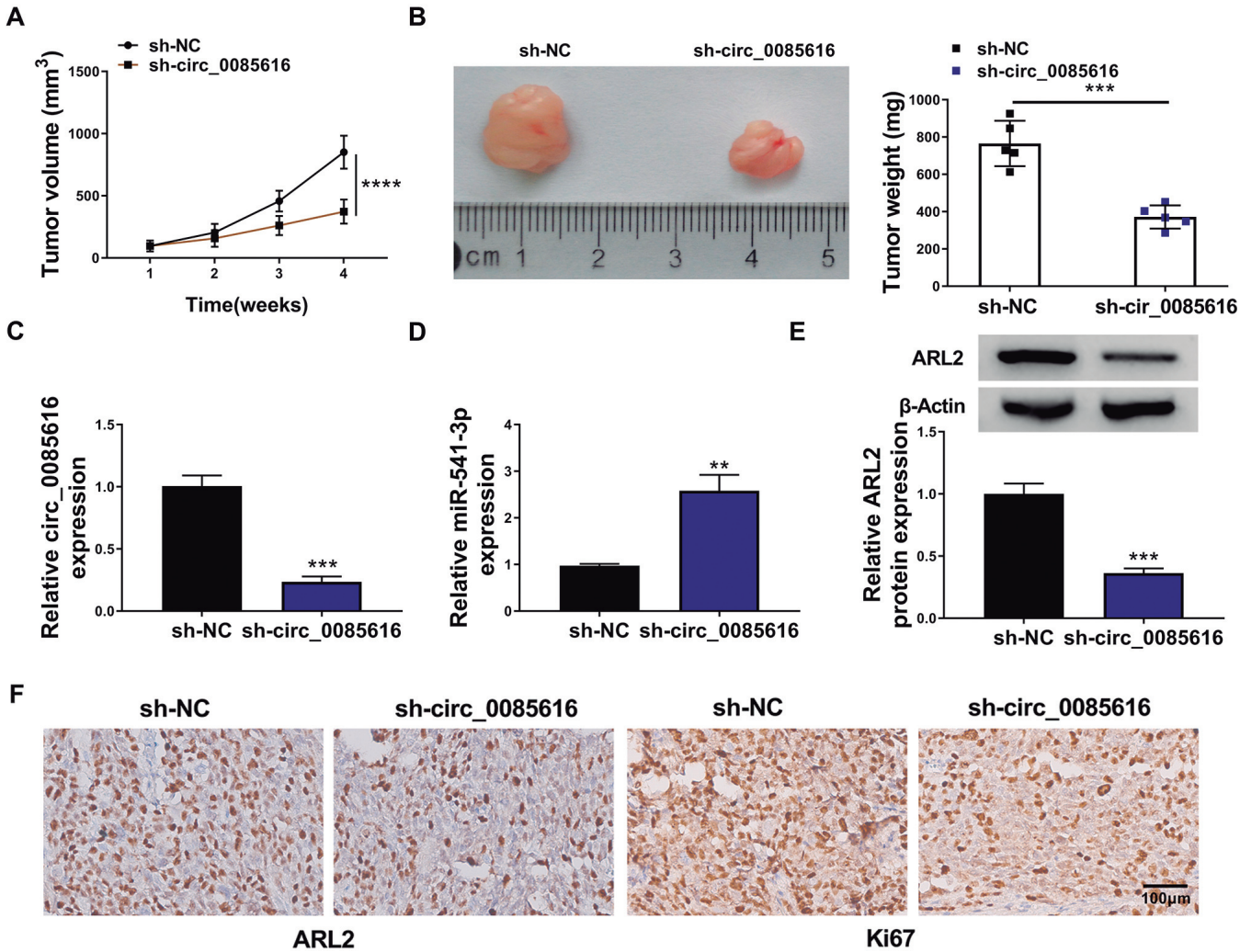

Fig. 11. Circ_0085616 silencing suppresses tumor growth *in vivo*. **A.** After injection for 1, 2, 3, or 4 weeks, the volume of xenograft tumors was measured as length×width^2×0.5. **B.** Four weeks after the injection, the nude mice were sacrificed, and the weight of xenograft tumors was recorded. **C, D.** RT-qPCR assay was conducted to measure the levels of circ_0085616 and miR-541-3p in xenograft tumor tissues. **E.** Western blot assay was employed to measure the protein level of ARL2 in xenograft tumor tissues. **F.** The levels of ARL2 and Ki67 in xenograft tumor tissues were determined by IHC assay. ***P*<0.01, ****P*<0.001, *****P*<0.0001.

CircRNAs can serve as oncogenic or tumor-suppressing factors in human malignancies (Zhang et al., 2018). Circ_0085616 is reported to contribute to the progression of hepatocellular carcinoma and cervical cancer. For instance, Li et al. claimed that circ_0085616 facilitates cell proliferation capacity and motility in hepatocellular carcinoma cells (Li et al., 2019). Lin et al. found that circ_0085616 abundance is elevated in cervical cancer, and it exhibits an oncogenic activity in cervical cancer by mediating the miR-503-5p/ATXN7L3 pathway (Lin et al., 2022). Consistently, it was found that circ_0085616 abundance was conspicuously enhanced in cervical cancer tissue specimens and cancer cell lines in our study. Subsequently, we explored the function of circ_0085616 in cervical cancer cells via silencing its level. Circ_0085616 knockdown prominently restrained the radio-resistance, proliferation, tube formation, and motility while it promoted cell apoptosis in cervical cancer cells.

The "miRNA sponge" role of circRNAs is embodied in circRNAs biology, which is responsible for the changes in cell biological behaviors and downstream genes (Hansen et al., 2013; Thomson and Dinger, 2016; Panda, 2018). The biological function of circRNAs is closely associated with their subcellular localization in cancer cells (Kristensen et al., 2019). It was observed that circ_0085616 was majorly distributed in the cytoplasm of cervical cancer cells, which suggested that circ_0085616 might serve as a miRNA sponge. Then, we found that circ_0085616 acted as a sponge for miR-541-3p. miR-541-3p played a tumor suppressor role in multiple malignancies, including prostate cancer (He et al., 2021), non-small cell lung cancer (Lu et al., 2016), and hepatocellular carcinoma (Xu et al., 2020). For example, miR-541-3p is reported to elevate cell radio-sensitivity in prostate cancer cells by reducing the abundance of HSP27 (He et al., 2021). This study is the first to evaluate miR-541-3p function in cervical cancer. miR-541-3p level was prominently reduced in cervical cancer tissue specimens and cancer cell lines. It was demonstrated that miR-541-3p overexpression suppressed the radio-resistance and malignant phenotypes of cervical cancer cells. Furthermore, circ_0085616 interference-mediated influences in cervical cancer cells were largely overturned by anti-miR541-3p, suggesting that circ_0085616 knockdown suppressed the radio-resistance and development of cervical cancer largely by up-regulating miR-541-3p.

miRNAs are well known to interact with target mRNAs at their 3'UTR, resulting in the degradation or the translational suppression of mRNAs (Ali Syeda et al., 2020). It was identified that miR-541-3p can interact with ARL2 3'UTR. ARL2 is reported to be targeted by several miRNAs, and it plays an oncogenic role in cervical cancer. For instance, miR-195-5p is reported to restrain the motility of cervical cancer cells by reducing ARL2 abundance (Pan et al., 2019). Chen et al. demonstrated that circ_0084927 contributes to cervical cancer progression by elevating ARL2 level via sponging miR-142-3p (Chen et al., 2020). We found that ARL2 overexpression largely reversed miR-541-3p overexpression-mediated impacts in cervical cancer cells, indicating that miR-541-3p overexpression inhibited cervical cancer development partly by down-regulating ARL2. Furthermore, we identified that circ_0085616 positively modulated ARL2 abundance by sequestering miR-541-3p.

Through a xenograft mouse model, we found that circ_0085616 knockdown conspicuously restrained tumor growth *in vivo*, and this suppressive effect was at least partly dependent on the modulation of miR-541-3p/ARL2 axis.

In conclusion, circ_0085616 played an oncogenic role in cervical cancer cells by elevating cell radio-resistance and malignant potential via the miR-541-3p/ARL2 axis, which provided novel potential targets for cervical cancer treatment.

Acknowledgements. None.

Ethics approval and consent to participate. Written informed consent was obtained from patients with approval by the Institutional Review Board in First Affiliated Hospital of Jinzhou Medical University.

Consent for publication. Not applicable.

Availability of data and materials. Please contact the correspondence author for data request.

Competing interests. The authors declare that they have no conflicts of interest

Funding. None.

Authors' contribution. Yan Tang was responsible for drafting the manuscript. Yan Tang and Kai Guo Lei Zhou contributed to the analysis and interpretation of data. Yan Tang and Lili Liu contributed in the data collection. All authors read and approved the final manuscript.

References

Ali Syeda Z., Langden S.S.S., Munkhzul C., Lee M. and Song S.J. (2020). Regulatory mechanism of microRNA expression incancer. Int. J. Mol. Sci. 21, 1723.

Chen L.L. and Yang L. (2015). Regulation of circRNA biogenesis. RNA Biol. 12, 381-388.

Chen L., Zhang X., Wang S., Lin X. and Xu L. (2020). Circ_0084927 facilitates cervical cancer development via sponging miR-142-3p and upregulating ARL2. Cancer Manag. Res. 12, 9271-9283.

Gao J.L., Chen G., He H.Q. and Wang J. (2018). CircRNA as a new field in human disease research. Zhongguo Zhong Yao Za Zhi. 43, 457-462 (in Chinese).

Guo J., Chen M., Ai G., Mao W., Li H. and Zhou J. (2019). Hsa_circ_0023404 enhances cervical cancer metastasis and chemoresistance through VEGFA and autophagy signaling by sponging miR-5047. Biomed. Pharmacother. 115, 108957.

Hansen T.B., Jensen T.I., Clausen B.H., Bramsen J.B., Finsen B., Damgaard C.K. and Kjems J. (2013). Natural RNA circles function as efficient microRNA sponges. Nature 495, 384-388.

He Z., Shen F., Qi P., Zhai Z. and Wang Z. (2021). miR-541-3p enhances the radiosensitivity of prostate cancer cells by inhibiting HSP27 expression and downregulating β-catenin. Cell Death Discov. 7, 18.

Hu Z.Q., Zhou S.L., Li J., Zhou Z.J., Wang P.C., Xin H.Y., Mao L., Luo C.B., Yu S.Y., Huang X.W., Cao Y., Fan J. and Zhou J. (2020). Circular RNA sequencing identifies CircASAP1 as a key regulator in hepatocellular carcinoma metastasis. Hepatology 72, 906-922.

Kristensen L.S., Andersen M.S., Stagsted L.V.W., Ebbesen K.K., Hansen T.B. and Kjems J. (2019). The biogenesis, biology and characterization of circular RNAs. Nat. Rev. Genet. 20, 675-691.

Kristensen L.S., Hansen T.B., Venø M.T. and Kjems J. (2018). Circular RNAs in cancer: opportunities and challenges in the field. Oncogene 37, 555-565.

Li H., Wu X. and Cheng X. (2016). Advances in diagnosis and treatment of metastatic cervical cancer. J. Gynecol. Oncol. 27, e43.

Li Z., Li Z., Wang L., Long C., Zheng Z. and Zhuang X. (2019). ZCCHC13-mediated induction of human liver cancer is associated with the modulation of DNA methylation and the AKT/ERK signaling pathway. J. Transl. Med. 17, 108.

Lin L., Li N., Hu X., Sun J. and He Y. (2022). Identification of circ_0085616 as an upregulated and oncogenic circular RNA in cervical xancer via the miR-503-5p-mediated ATXN7L3 activation. Cancer Biother. Radiopharm. (in press)

Lu Y.J., Liu R.Y., Hu K. and Wang Y. (2016). MiR-541-3p reverses cancer progression by directly targeting TGIF2 in non-small cell lung cancer. Tumour Biol. 37, 12685-12695.

Masadah R., Rauf S., Pratama M.Y., Tiribelli C. and Pascut D. (2021). The role of microRNAs in the Cisplatin- and radio-Resistance of cervical cancer. Cancers (Basel). 13, 1168.

Matozaki T., Nakanishi H. and Takai Y. (2000). Small G-protein networks: their crosstalk and signal cascades. Cell. Signal. 12, 515-524.

Meng S., Zhou H., Feng Z., Xu Z., Tang Y., Li P. and Wu M. (2017). CircRNA: functions and properties of a novel potential biomarker for cancer. Mol. Cancer 16, 94.

Pan S.S., Zhou H.E., Yu H.Y. and Xu L.H. (2019). MiR-195-5p inhibits the cell migration and invasion of cervical carcinoma through suppressing ARL2. Eur. Rev. Med. Pharmacol. Sci. 23, 10664-10671.

Panda A.C. (2018). Circular RNAs act as miRNA sponges. Adv. Exp. Med. Biol. 1087, 67-79.

Pu M., Chen J., Tao Z., Miao L., Qi X., Wang Y. and Ren J. (2019). Regulatory network of miRNA on its target: coordination between transcriptional and post-transcriptional regulation of gene expression. Cell Mol. Life Sci. 76, 441-451.

Shao S., Wang C., Wang S., Zhang H. and Zhang Y. (2020). Hsa_circ_0075341 is up-regulated and exerts oncogenic properties by sponging miR-149-5p in cervical cancer. Biomed. Pharmacother. 121, 109582.

Tang Q., Chen Z., Zhao L. and Xu H. (2019). Circular RNA hsa_circ_0000515 acts as a miR-326 sponge to promote cervical cancer progression through up-regulation of ELK1. Aging (Albany NY). 11, 9982-9999.

Thomson D.W. and Dinger M.E. (2016). Endogenous microRNA sponges: evidence and controversy. Nat. Rev. Genet. 17, 272-283.

Wang Y., Guan G., Cheng W., Jiang Y., Shan F., Wu A., Cheng P. and Guo Z. (2018). ARL2 overexpression inhibits glioma proliferation and tumorigenicity via down-regulating AXL. BMC Cancer 18, 599.

Xu Q., Zhou L., Yang G., Meng F., Wan Y., Wang L. and Zhang L. (2020). CircIL4R facilitates the tumorigenesis and inhibits ferroptosis in hepatocellular carcinoma by regulating the miR-541-3p/GPX4 axis. Cell Biol. Int. 44, 2344-2356.

Zhang H.D., Jiang L.H., Sun D.W., Hou J.C. and Ji Z.L. (2018). CircRNA: a novel type of biomarker for cancer. Breast Cancer 25, 1-7.

Accepted October 27, 2022